# DIGITALES ARCHIV

Alvarino, Natalia Ivaneth Luna; Santos, Vladimir Sousa; González, Jairo Ricardo

Article

# Design of photovoltaic systems in industrial electrical systems considering power quality

International Journal of Energy Economics and Policy

This Version is available at:
http://hdl.handle.net/11159/653630

Mitglied der

Leibniz-Gemeinschaft

# Design of Photovoltaic Systems in Industrial Electrical Systems Considering Power Quality

# Natalia Ivaneth Luna Alvarino[1], Vladimir Sousa Santos[2]*, Jairo Ricardo González[3]

[1]Student of the Electrical Engineering Program, Universidad de la Costa, Barranquilla, Colombia, [2]Department of Energy, Universidad de la Costa, Barranquilla, Colombia, [3]JR Montajes y Soluciones de Ingeniería S.A.S., Barranquilla, Colombia. *Email: vsousa1@cuc.edu.co

## ABSTRACT

This paper presents a comprehensive design methodology for photovoltaic systems (PVS) integrated into industrial electrical systems (IES), with a specific focus on preserving power quality (PQ). The 10-step methodology, ranging from initial interviews to detailed technical, energy, and economic assessments, is novel for its multi-factorial approach that combines an Excel application with ETAP software, prioritizing considerations for PQ. Evaluation across four scenarios demonstrated varying outcomes. In the worst-case technical and energy scenario, PVS installation on Point of Common Connection without PQ mitigation led to significant increases in harmonics and no reduction in energy consumption. Conversely, the best technical and energy scenario involved distributing PVS across load buses with PQ mitigation, resulting in a 5% reduction in energy consumption and 27% lower energy losses. The economic evaluation indicated a 3-year payback period in all scenarios, primarily attributed to increased costs for PQ problem mitigation equipment. It was also observed that reducing losses and energy consumption limits the economic benefits of installing PVS in IES. This methodology serves as a valuable guide for designing PVS in IES, incorporating technical, energy, economic, and PQ considerations.

**Keywords:** Distributed Generation, Industrial Electrical System, Photovoltaic Systems, Power Quality, Project Feasibility Evaluation
**JEL Classifications:** L8, Q2, Q4

## 1. INTRODUCTION

The unprecedented economic growth of the 21st century has led to a surge in global energy demand, creating an urgent need to balance energy supply and demand (Ren et al., 2021). In this context, utility companies are facing increasing pressure to meet the growing demand for electricity (Jamil et al., 2019), and traditional energy sources are struggling to meet modern energy demands, raising concerns about reliability, safety, and environmental impact (Khare et al., 2016). Countries like China, with a significant portion of energy consumption in the electric industry, encounter challenges stemming from outdated distribution network infrastructure, resulting in energy losses (Ahmad et al., 2021).

As a result, there is an urgent need to enhance energy efficiency and reduce losses in the distribution network (Adefarati and Bansal, 2019). To address these challenges, there is a growing momentum in the utilization of renewable and distributed energy sources, especially Renewable Energy Hybrid Systems based on Distributed Energy Resources (Sinha & Chandel, 2017). Hybrid systems combining solar photovoltaic and wind energy, leveraging the complementary nature of solar and wind power, have garnered worldwide attention for their potential to improve energy supply reliability (Sharma et al., 2019).

The power generation capacity with photovoltaic systems (PVS) reaching 1171 GW by the end of 2022 (Global Status Report, 2021), reflects the growing significance of renewable energy.

However, the incorporation of renewable energy sources into the electrical grid necessitates an inclusive energy planning strategy that incorporates demand-side management. This approach is essential to guarantee the stability of system voltage and frequency (Cabana-Jiménez et al., 2024). Simultaneously, the industrialization, urbanization, and increasing demand for electricity raise concerns about power quality (PQ) (Angarita et al., 2023), (Choudhury, 2022). The intermittent nature of renewable sources can impact power system stability, causing various issues such as voltage dips, harmonics, voltage swells, slow voltage variations, voltage imbalances, transients, frequency variations, fast voltage variations, and unnecessary reactive power generation (Charris et al., 2023; Saqib and Saleem, 2015).

While existing literature delves into the design and optimization of renewable energy systems, particularly PVS, a common limitation is the limited consideration of PQ. For instance, (Al-Karakchi et al., 2019) focuses on a cost-effective design for a combined PVS with electrical energy storage, catering to remote communication infrastructure. Similarly, (Ali et al., 2019) proposes an economical photovoltaic water pumping system with maximum power point tracking (MPPT), emphasizing the significance of the MPPT algorithm, and (Zidane et al., 2019) computes the Levelized Cost of Electricity for different PVS topologies.

In (Roy et al., 2019), a PVS with a battery using perturb and observe MPPT technique is discussed, emphasizing cost-effectiveness, while (Yang et al., 2023) incorporates a hybrid multi-criteria decision-making method for risk management in PVS design projects. In (Barbón et al., 2023) an optimization methodology for single-axis PVS plants is presented, (Ren et al., 2023) proposes a comprehensive solution to grid connection and abandonment issues in wind and PVS, and (Koholé et al., 2023) provides a techno-economic comparison and optimal design of PV/wind hybrid systems for rural electrification.

In (Nasir et al., 2023), a hybrid configuration of pumped storage hydropower, floating PVS, and conventional hydropower is explored, (Naderipour et al., 2022) focuses on the optimal design of a grid-connected PV-wind energy system with battery storage, and (Habib et al., 2023) discusses an optimally designed solar PV water pumping system considering factors like water requirement and solar resources. Despite these valuable insights, there is a gap in examining PQ aspects in the design and optimization of renewable energy systems in industrial electrical systems (IES).

This paper aims to address this gap by presenting a methodology for designing PVS in IES that considers the PQ. The novelty of the proposed methodology is its multifactorial approach since it is based on the use of an application developed in Excel in conjunction with modeling in the ETAP electrical modeling software. The methodology allows to comprehensively evaluate the factors that are commonly considered in PVS designs, such as the load graphs and the energy that is desired to be supplied from these sources, with other more specific factors of the operation of the IES, such as the location of the PVS in the IES, the PQ, energy losses and associated costs.

Section II of the article describes the steps of the methodology, providing a comprehensive guide to its application. Section III evaluates the methodology through a case study, offering practical insights into its effectiveness. Finally, Section IV presents the conclusions drawn from the study, summarizing the key findings and their implications for the design of PVS. The incorporation of PQ considerations in the design process enhances the overall understanding and performance of these systems, contributing to sustainable and reliable energy solutions.

## 2. MATERIALS AND METHODS

The methodology proposed in this research for the design of PVS in IES considering the PQ is based on the use of an application developed in Excel in conjunction with the modeling of the IES in the ETAP electrical modeling software. This methodology is represented in the flow chart in Figure 1.

The steps of the methodology are described below:

**Figure 1:** Flowchart of PVS design methodology considering PQ
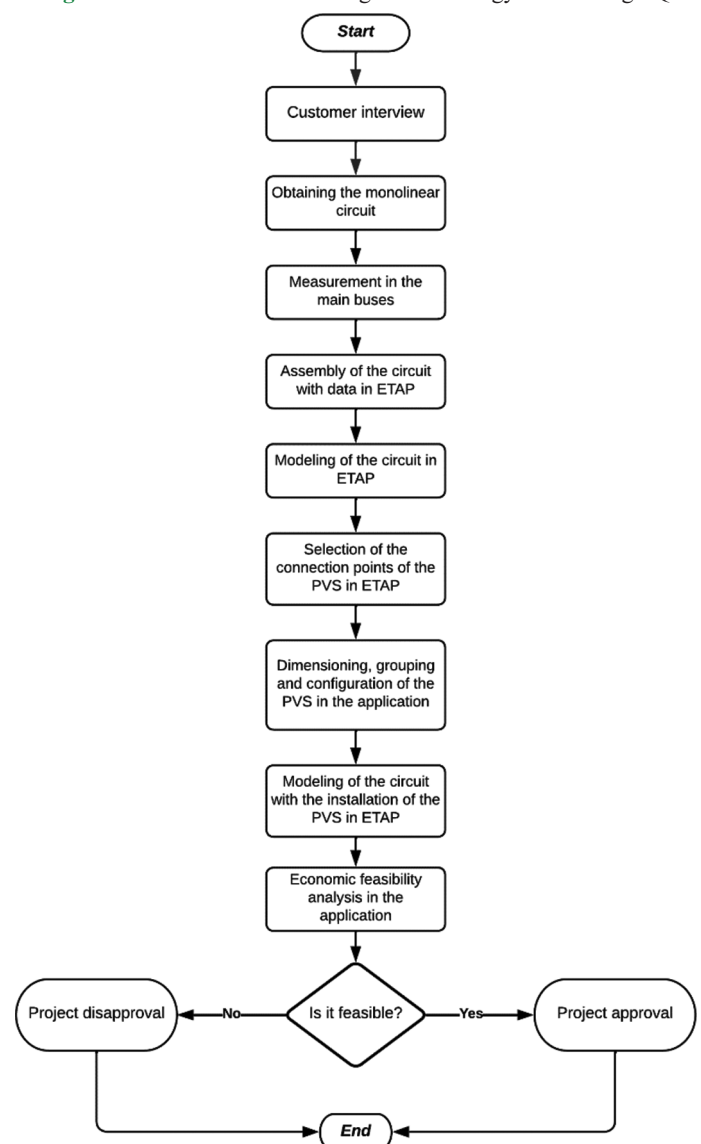
## 2.1. Interview with the Company Client Interested in the Installation of the PVS

The purpose of this step is to learn about the company's interests, as well as to request information about the IES and energy consumption. It also includes a tour of the company's electrical system to identify the points of measurement of electrical parameters and the possible points of connection of the PVS.

## 2.2. Obtaining the Monolinear Circuit

The monolinear circuit is delivered by the company, and it must be verified that the circuit configuration and the data of the components and equipment are up to date.

## 2.3. Measurement of the Load and PQ Parameters on the Main Bus and Load Buses

The measurements must be carried out with a network analyzer for a week with recording intervals that do not exceed 10 min according to the recommendations of the IEEE Std 1159™-2019 (IEEE Std 1159, 2019). Among the parameters that must be measured are voltages, currents, power factor, active, reactive, and apparent powers, as well as total and individual harmonics of voltage and current.

## 2.4. Assembly of the Monolinear Circuit with the Data of the Parameters in the ETAP Software

In this step, the assembly of the monolinear circuit is carried out in the ETAP software based on the data provided by the company and the measurements made.

## 2.5. Modeling of the Circuit in ETAP

In this stage, the initial IES is modeled and characterized in the ETAP software through the following studies:

- Load flow
- Short circuit analysis
- Harmonic analysis
- Unbalanced load flow.

In these studies, the limits established by Standards NTC 1340 (ICONTEC, 2013), IEEE Std 1159™-2019 (IEEE Std 1159, 2019) and NTC 5001:2008 (ICONTEC, 2008) are considered.

## 2.6. Selection of the Connection Points of the Photovoltaic Systems in the Monolineal Circuit

For the evaluation of the PVS design, it is suggested to compare the behavior of the IES and the associated costs when the PVS is connected to the PCC or to the load buses.

## 2.7. Dimensioning, Grouping, and Configuration of the PVS

For the dimensioning, grouping, and configuration of the PVS, the parameters considered encompass the features of the IES, measurements obtained, and specifications of the solar panels and inverters slated for implementation. Essential data for this analysis includes:

- Power demanded by the electrical system, corresponding to the maximum power recorded in the load graph.
- Nominal network voltage.
- Power to install.
- Characteristic data of the three-phase DC-AC inverter: Nominal output power according to demand and inverter capacity, maximum input voltage, voltage range for MPPT, maximum input current, inverter efficiency and input power.
- Characteristic data of the selected PV module: Nominal power, short circuit current, open circuit voltage and module surface.

The equations that allow the dimensioning, grouping and configuration of the PVS are described below (Corporación de desarrollo Tecnológico-Cámara chilena de construcción, 2013):

The PV modules are primarily composed of photovoltaic panels and an inverter. The number of photovoltaic panels per module depends on the maximum power of the inverter and is calculated as follows:

$$N = \frac{0.85 * P_{maxinv}}{P_{peak}} \tag{1}$$

Where N is the number of photovoltaic panels, $P_{maxinv}$ is the maximum power of the inverter (kW), and $P_{peak}$ is the peak power of the selected photovoltaic panel (kW).

The factor of 0.85 ensures that the maximum power of the inverter is 1.15 times greater than the maximum power that the solar panels can deliver, in accordance with the recommendations of (Corporación de desarrollo Tecnológico-Cámara chilena de construcción, 2013). The number of photovoltaic panels that can be connected in series is calculated as:

$$N_s = \frac{Vmax_{inv}}{V_{oc}} \tag{2}$$

Where: Ns is the maximum number of photovoltaic panels in series, $Vmax_{inv}$ is the maximum input voltage of the inverter (V), and $V_{OC}$ is the open-circuit voltage of the selected photovoltaic panel (V).

The number of photovoltaic panels that can be connected in parallel is calculated as

$$N_P = \frac{Imax_{inv}}{I_{sc}} \tag{3}$$

Where: Np is the maximum number of photovoltaic panels in parallel, $Imax_{inv}$ is the maximum input current of the inverter (A), and $I_{SC}$ is the short-circuit current of the selected photovoltaic panel (A).

The open-circuit voltage, short-circuit current, and power that each PVS module can deliver are calculated using equations (4), (5), and (6). These parameters must be equal to or less than $Vmax_{inv}$, $Imax_{inv}$ and $Pmax_{inv}$

$$V_{ocPVS} = V_{oc} \cdot N_S \tag{4}$$

Where $V_{OCPVS}$ is the open-circuit voltage of the PVS (V).

$$I_{scPVS} = I_{sc} \cdot N_P \tag{5}$$

Where I $I_{scPVS}$ is the short-circuit current of the PVS (A).

$$P_{FV} = P_{pico} \cdot N \tag{6}$$

Where: $P_{FV}$ is the output power of the PVS module (kW)

The area that a PVS module will occupy is calculated by applying the following equation:

$$S_T = N \cdot A \tag{7}$$

Where: $S_T$ is the surface area required for the installation of the PVS (m²), and A is the surface area of one module (m²).

The total number of required PVS modules, i.e., the inverter with the arrays of solar panels, is calculated based on the maximum power intended to be supplied to the IES as follows:

$$NM_{PVS} = \frac{P_{max}}{P_{FV}} \tag{8}$$

Where $NM_{PVS}$ is the quantity of PVS modules, and $P_{max}$ is the maximum power demand of the IES (kW).

## 2.8. Modeling of the Circuit with the Installation of the PVS in ETAP

In this step, the same studies as in step five are conducted, considering various analysis scenarios of the circuit under study, including the connection of the PVS.

## 2.9. Analysis of the Economic Feasibility of PVS Configuration Alternatives and Mitigation of PQ Problems

In this section, an economic feasibility analysis of the PVS is conducted, utilizing the life cycle cost (LCC) and net present value (NPV) methods, based on the following costs associated with the installation and operation of the PVS (Ndwali et al., 2020):

- Initial investment cost ($k_0$): Encompasses the cost of purchasing and installing the PVS and additional accessories such as cables and protection devices, among others. The initial investment cost is calculated as:

$$k_0 = IC_{FV} + IC_{inv} \tag{9}$$

Where: ICFV is the initial cost of photovoltaic panels (COP), and $IC_{in}$ is the cost of inverters (COP).

- Operation and Maintenance Costs ($C_{O\&M}$): Encompasses the cost of operating and maintaining the PVS.
- Replacement Costs ($C_r$): These costs represent the expense of replacing components with a limited lifespan. For inverters, this cost is calculated as:

$$C_r = \frac{C_{inv}}{UL_{inv}} \tag{10}$$

Where: Cr is the replacement cost, $C_{inv}$ is the initial cost of the inverter, and $UL_{inv}$ is the useful life of the inverter.

- Costs due to electrical losses, including Joule and PQ losses ($C_{EL}$): These costs are calculated as the product of electrical losses, including losses from PQ issues, multiplied by the cost of energy. Electrical losses are calculated as the difference between the total power demanded by the IES at the PCC and the power demanded by the installed loads.

The life cycle cost is calculated as:

$$LCC = k_0 + C_{O\&M} + C_r + C_{EL} \tag{11}$$

Where: LCC is the life cycle cost (COP).

The Net Present Value is calculated as:

$$NPV = -k_0 + \sum_{i=1}^{n} \frac{Cf_i}{(1+D)^i} \tag{12}$$

Where: VPN is the net present value (COP), n is the project's useful life (years), i is the current year, $Cf_i$ is the cash flow (COP), and D is the discount rate (p.u).

The cash flow is calculated as:

$$Cf_i = I_i - G_i \tag{13}$$

Where: $I_i$ is the income (COP), and $G_i$ is the expenses (COP).

Expenses include costs associated with the operation of the PVS and the IES, such as operation and maintenance costs, replacement costs, and costs due to electrical losses, including losses from PQ.

Income consists of the annual energy supplied by the PVS to the IES, which is consequently billed to the energy supply companies. The other component of income is the surplus energy that can be delivered and marketed to the electrical supply network. The costs of energy marketed by energy supply companies to end-users generally differ from the cost of surplus energy generated from unconventional renewable energy sources, which end-users can market to energy supply companies (XM, 2024).

Income is calculated using the following equations:

$$I_i = GE_{PVS} \cdot C_E + GE_{exc} \cdot C_{Eexc} \tag{14}$$

Where: $GE_{PVS}$ is the annual energy generation from the PVS (kWh/year), GEexc is the annual surplus energy generation from the PVS (kWh/year), $C_E$ is the cost of energy (COP), and $C_{Eexc}$ is the cost of surplus energy that can be marketed to the grid from the PVS (COP).

## 2.10. Definition of the Best Photovoltaic System Design Solution Considering the PQ

The optimal design of the PVS can be defined using the application based on the identification of scenarios with lower energy losses, lower life cycle costs, and higher Net Present Value.

# 3. RESULTS

## 3.1. Initial Conditions of the IES under Study

The methodology based on the application to design PVS considering PQ issues was validated in an IES. The IES features two transformers: One with a capacity of 1000 kVA, operating at 13.2 kV/480 V, which constitutes the PCC; and the other with a

capacity of 112.5 kVA, operating at 480 V/240 V, supplying power to single-phase loads. Figure 2 depicts the single-line diagram of the IES, while Figure 3 illustrates the load profile of the IES at the PCC during a typical working day.

In the 480 V circuit, nine three-phase electric motors are powered. Out of these nine motors, three 30 HP motors drive centrifugal pumps (BUS_3), three 25 HP motors drive compressors (BUS_4), and three 40 HP motors drive fans (BUS_5). In the 240 V circuit, single-phase lighting loads of 24 kW and air conditioning loads of 36 kW are supplied (BUS_6).

This IES is characterized by an increase in the size of the electric motors for centrifugal pumps and compressors due to the expansion of production capacity. Additionally, new air conditioning units were added to accommodate the growth in the administrative area. Furthermore, the electric motors and the air conditioning system are controlled by six-pulse frequency inverters, while the lighting system uses fluorescent lighting. Additionally, the circuits of the lighting and air conditioning systems are distributed across phases AB.

Table 1 displays the power demanded by the loads, the total power, and losses in the circuit due to Joule effects and PQ issues. It also presents parameters related to PQ (voltage variation, voltage imbalance, and harmonics), as well as factors such as power factor, short-circuit current, maximum current, and the short-circuit current to maximum current ratio used for harmonic current analysis. These parameters were obtained from the analysis of load flow, short circuit, harmonic, and unbalanced load implemented in the ETAP software.

In Table 1, parameters exceeding the PQ limits set by standards are highlighted in red. According to Table 1, the IES exhibits a low power factor at the load buses BUS_3, BUS_4, BUS_5, and at the main bus (PCC), as the values are below the 90% limit established by standard (CREG, 2018). Additionally, there are issues of low voltage at buses BUS_3, BUS_5, and BUS_6, as the voltage variation is below 92%, a limit set by standard (ICONTEC, 2013) for circuits with voltages below 1000 V. Table 1 also reveals voltage imbalance issues at BUS_6, as it has a value of 7.1%, exceeding the 2% limit established by standard (IEEE Std 1159, 2019).

The table also highlights problems related to voltage and current harmonics. Total harmonic distortion of voltage exceeds 8% at BUS_3, while individual harmonics of voltage of order 5 surpass the 5% limit established by standard (IEEE, 2014) at buses BUS_3 and BUS_5. Considering the short-circuit current to maximum current ratio (ICC/Imax) falls within the range of 20-50 with a

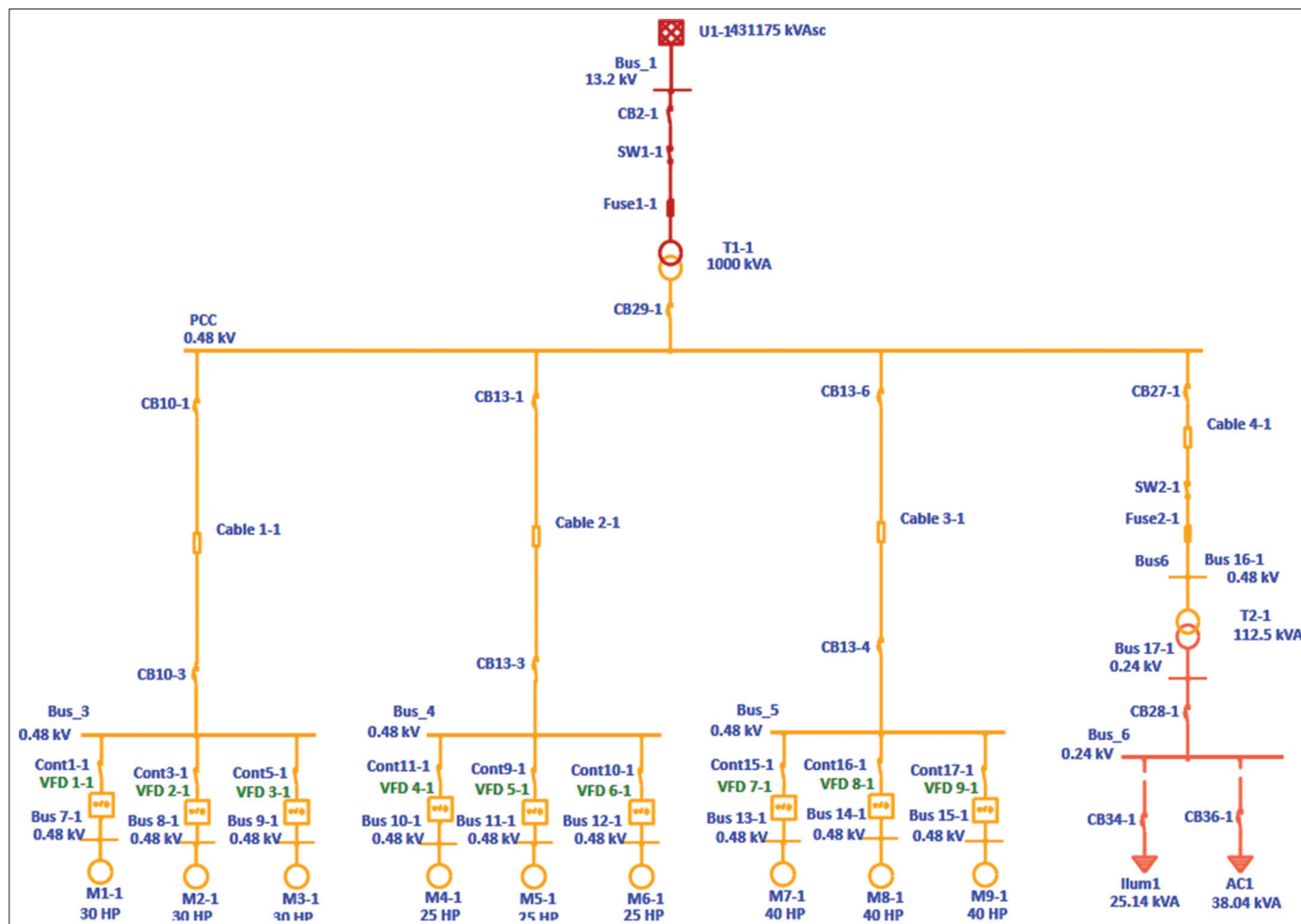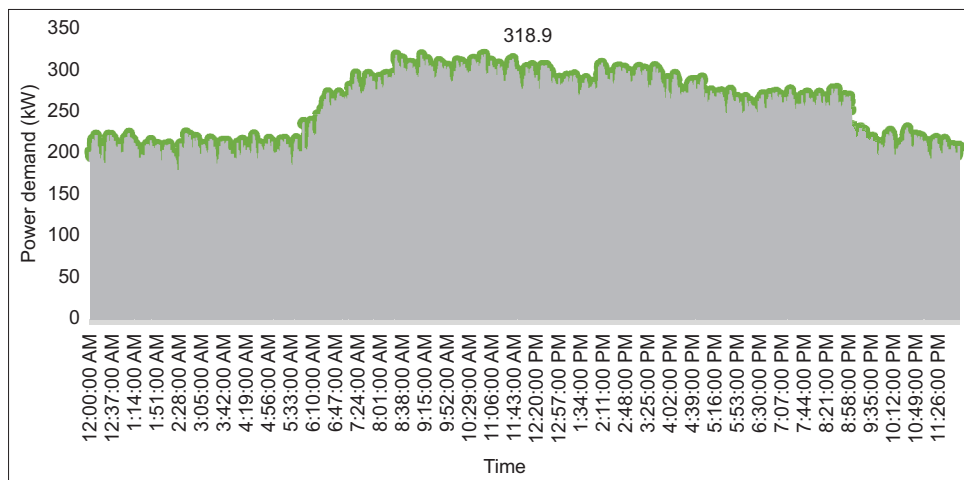**Figure 2:** Single-line diagram of the IES under study

**Figure 3:** Load profile at the PCC



**Table 1: Electrical parameters of the initial condition on IES**

| Parameters | PCC | Bus_3 | Bus_4 | Bus_5 | Bus_6 |
|---|---|---|---|---|---|
| Total power (kW) | 318.9 | N/A | N/A | N/A | N/A |
| Power demand by loads (kW) | 295.0 | N/A | N/A | N/A | N/A |
| Total power losses (kW) | 24.0 | N/A | N/A | N/A | N/A |
| PF (%) | 76 | 69 | 68 | 81 | 94 |
| Voltage variation (%) | 98.3 | 89.8 | 95.8 | 90.7 | 91.2 |
| Voltage imbalance (%) | 0.2 | 0.4 | 0.3 | 0.3 | 7.1 |
| ICC (A) | 24.765.0 | N/A | N/A | N/A | N/A |
| Imax (A) | 508.2 | 155.0 | 122.1 | 168.6 | 69.3 |
| ICC/imax | 48.7 | N/A | N/A | N/A | N/A |
| THD V (%) | 2.3 | 9.5 | 4.1 | 7.9 | 4.3 |
| TDD (%) | 17.6 | 22.9 | 23.9 | 23.2 | 14.1 |
| V5 (%) | N/A | 6.92 | 3.24 | 6.06 | 3.12 |
| V7 (%) | N/A | 2.42 | 1.13 | 1.96 | 1.40 |
| V10 (%) | N/A | 2.55 | 1.07 | 1.70 | 1.03 |
| V12 (%) | N/A | 2.69 | 1.10 | 1.61 | 1.32 |
| I5 (%) | N/A | 21.38 | 22.22 | 21.59 | 13.35 |
| I7 (%) | N/A | 5.54 | 5.76 | 5.64 | 3.39 |
| I10 (%) | N/A | 4.20 | 4.37 | 4.31 | 2.25 |
| I12 (%) | N/A | 3.87 | 4.03 | 3.98 | 1.65 |

Where: N/A indicates data not applicable, PF is the power factor, ICC is the short-circuit current, Imax is the maximum demanded current, THDV is the total harmonic distortion of voltage, TDD is the total demand distortion, VK is the individual harmonic of voltage of order K, and IK is the individual harmonic of current of order K

value of 48.7, the total demand distortion exceeds the 4% limit at the PCC set by standard (IEEE, 2014). Additionally, individual harmonics of current of order 5 exceed the 3.5% limit at all load buses, and individual harmonics of current of order 12 surpass the 1.75% limits at load buses BUS_3, BUS_4, and BUS_5 according to standard (IEEE, 2014).

The issues of low power factor and voltage variation result from the increased load in the IES, voltage imbalance is due to the unequal distribution of single-phase loads, and harmonics are caused by the six-pulse frequency inverters. These problems contribute to the 24 kW electrical losses present in the IES.

Table 2 displays data on energy consumption and associated costs. Annual energy consumption is determined from the IES load curve (Figure 2), considering that the company operates 24 h a day, 300 days a year. Costs associated with energy consumption are calculated considering a cost of 1000 COP/kWh (XM, 2024).

From Table 2, it can be inferred that energy losses due to Joule effects and PQ issues represent 17.9% of the total energy consumption. The energy consumption during the period from 9 a.m. to 4 p.m. from the electrical grid (619,467 kWh/year) will be supplied by the PVS since, during this time frame, solar radiation in the study area varies between 378 W/m² and 884 W/m² (Tutiempo Network, n.d.). This implies an annual savings of 495,573,543 COP and a 33.9% reduction in total energy consumption.

### 3.2. Scenario Evaluation using the Application
Starting from the analysis of the IES in its initial condition, where PQ issues are evident, the implementation of the application is assessed for the installation of PVS in the following scenarios:
1. Installation of PVS at the PCC without improving PQ
2. Installation of PVS at the PCC while improving PQ
3. Installation at the load buses without improving PQ
4. Installation at the load buses while improving PQ.

In scenarios 1 and 3, the PVS design focuses solely on supplying the energy that the company consumes from the electrical grid during the period from 9 a.m. to 4 p.m, using basic PVS components. In scenarios 2 and 4, in addition to achieving the goal of replacing the energy consumed from the electrical grid, efforts are made to mitigate PQ issues. In these conditions, pure sine wave inverters, harmonic filters, and load balancing in circuits supplying single-phase loads were used. In scenarios 1 and 2, the installation of PVS was projected at the PCC, as commonly done in such projects (Ali et al., 2019), (Zidane et al., 2019), (Roy et al., 2019), while in scenarios 3 and 4, the installation was projected at the load buses. Table 3 summarizes the characteristics of the technologies and procedures applied in each scenario.

For establishing a baseline reference for scenario comparison, solar panels with identical characteristics and inverters of equal power were utilized, with the distinction that one is standard, and the other is pure sine wave. The harmonic filters, in turn, are of the simple tuned passive type and enable power factor correction. To perform load balancing, the reconnection between phases of the circuits was simulated, ensuring that the current in each phase is approximately equal. Table 4 displays the characteristics of the solar panels, and Table 5 presents the data for the inverters.

Table 6 presents the data for the harmonic filters, while Table 7 shows the quantity of modules (inverter and panels) and arrays (series and parallel connection) in the PVS. The harmonic filters were sized using the ETAP program, applying the procedure described in (Abril, 2012), primarily focusing on mitigating 5th-order harmonics and raising the power factor to 0.96 at the load buses. The configurations of the PV arrays were obtained using the application in Excel based on load graphs and data from the components of the PVS.

Table 7 indicates that in scenarios 2, 3, and 4, one module less is used than in scenario 1. This is because in scenario 2, the power demand from the IES is reduced due to the mitigation of PQ issues, while in scenarios 3 and 4, power demand is reduced due to the positive effect of distributed generation from the PVS at the load buses. In scenarios 3 and 4, even though the same number of modules is used, the difference lies in scenario 4 using pure sine wave inverters in the PVS and including harmonic filters with the data shown in Table 6. Figure 4 presents the power factor and PQ parameters (voltage variation, voltage imbalance, total voltage harmonic distortion, and total demand distortion) at the PCC and load buses.

Figure 4 illustrates that at the PCC and at the load buses, the initially low power factor is improved in scenarios 3 and 4, where harmonic filters are installed. This improvement is attributed to the fact that these filters also allow for the reduction of inductive reactive power. Additionally, an increase in total voltage and current harmonics is observed when PVS is installed without considering PQ issues (i.e., scenarios 1 and 3), as conventional inverters with nonlinear characteristics were used in these scenarios.

In (Figure 4a), it is observed that with the installation of PVS at the PCC, THD quintuples at the main bus, and when PVS is installed at the load buses, THDV triples compared to the initial conditions. Similarly, (Figure 4a) shows that current harmonics at the PCC, analyzed through TDD, increase by a factor of 2.4 with the installation of PVS at the PCC, while with the installation of PVS at the load buses, TDD increases by a factor of 1.9 compared to initial conditions. These harmonics are adequately mitigated in scenarios where harmonic filters are deployed (i.e., scenarios 2 and 4).

In (Figure 4b, d, e), it is demonstrated that the initially low voltage at buses 3, 5, and 6, respectively, is improved in scenarios where PVS are distributed at the load buses (i.e., scenarios 3 and 4) and where harmonic filters are installed (i.e., scenarios 2 and 4). These improvements are attributed to the fact that generation close to consumption points reduces losses causing voltage drop, and harmonic filters allow voltage increase due to capacitive reactive power generation. In fact, in scenario 2, even though the PVS is placed at the PCC, the voltage increases due to the positive effect of the harmonic filters.

**Table 2: Energy consumption and associated costs in the IES**

| Parameters | PCC |
| --- | --- |
| Total energy consumption (kWh/year) | 1,826,276.6 |
| Load energy consumption (kWh/year) | 1,499,335.5 |
| Energy consumption (9 a.m. to 4 p.m.) (kWh/year) | 619,467 |
| Total energy losses (kWh/year) | 326,941.1 |
| Costs for energy consumption (COP/year) | 1,826,276,595 |
| Costs for total energy losses (COP/year) | 326,941 |
| Costs for energy consumption (9 a.m. to 4 p.m.) (COP/year) | 619,466,928 |

Where: COP stands for Colombian pesos

**Table 3: Characteristics of PVS design in each scenario**

| Scenarios | PVS at the PCC | PVS at load buses | PVS with standard inverter | PVS with pure sine wave inverter | Harmonic filters | Load balancing |
| --- | --- | --- | --- | --- | --- | --- |
| 1 | X | | X | | | |
| 2 | X | | | X | X | X |
| 3 | | X | X | | | |
| 4 | | X | | X | X | X |

"X" indicates the presence of the specified feature or design in each scenario

Regarding the voltage unbalance observed at BUS_6 (Figure 4e) due to uneven distribution of single-phase loads, it improves in scenarios where load redistribution is carried out (scenarios 2 and 4).

Figure 5 presents the energy consumption of the IES in the loads, as well as losses caused by Joule effect and PQ issues. Additionally, Figure 5 shows the energy generated by the PVS, consumed by the IES from the PVS, and the surplus energy delivered to the electrical grid.

Figure 5 shows that in scenario 1, placing PVS at the PCC without mitigating PQ issues has no impact on energy consumption or energy losses. In scenario 2, on the other hand, placing PVS at the PCC while mitigating PQ issues results in a 2% reduction in energy consumption and a 13% reduction in energy losses. In scenario

3, installing PVS in a distributed manner near load connection points reduces energy consumption by 3% and energy losses by 16%. The optimal technical and energy scenario is scenario 4, where PV generation is distributed at load buses, eliminating PQ issues, and achieving a 5% reduction in energy consumption and a 27% reduction in losses caused by Joule heating and power quality issues.

Additionally, Figure 5 demonstrates that using a greater number of PV modules in scenario 1, compared to the other scenarios, allows for greater energy generation from PVS. In scenario 1, the highest energy consumption (i.e., 693,000 kWh/year) occurs during peak solar radiation hours (i.e., from 9:00 am to 4:00 pm), enabling a greater benefit from renewable energy use. Conversely, scenario 4, being the most energy-efficient, allows for a less extensive use of energy from PVS, with 589,105 kWh/year.

Regarding surplus energy that the PVS can deliver to the electrical grid, Figure 5 highlights that the highest amount is achieved in scenario 1 with 73,543 kWh/year because it has the greatest generation potential, while the lowest surplus is obtained in scenario 2, where PV generation aligns most closely with IES consumption during the 9:00 am to 4:00 pm timeframe.

Table 8 and Figure 6 present the results of the economic feasibility of the analyzed scenarios in the case study. Table 8 displays the costs of investment, energy consumption, energy losses, operation, maintenance, and replacement. It also includes income from PVS generation, and the sale of surplus energy generated by PVS. Figure 6 illustrates the life cycle cost and the payback period for each scenario.

### Table 4: Solar panel data

| Parameters | Values |
|---|---|
| Power (W) | 239.7 |
| Short-circuit current (A) | 8.33 |
| Open-circuit voltage (V) | 37.08 |
| Efficiency (%) | 14.9 |
| Dimensions (length×width) (m) | 1.65×0.982 |

### Table 5: Inverter data used in the PVS

| Parameters | Values |
|---|---|
| Nominal power (W) | 30,000 |
| Maximum input voltage (V) | 1,000 |
| Maximum input current (A) | 48 |
| Efficiency (%) | 98.2 |
| Voltage range at maximum power point | (250-960) V |

### Table 6: Harmonic filter data for each scenario

| Scenarios | Harmonic filter data | | | | |
|---|---|---|---|---|---|
| | PCC | BUS-3 | BUS-4 | BUS-5 | BUS-6 |
| 1 | N/A | N/A | N/A | N/A | N/A |
| 2 | N/A | Q=66.37 kVAR C=764.1 µF XL=0.1389 Ω R=0.0015 Ω V=480 V | Q=53.33 kVAR C=614 µF XL=0.1728 Ω R=0.0015 Ω V=480 V | Q=48.32 kVAR C=556.4 µF XL=0.1907 Ω R=0.0015 Ω V=480 V | Q=3.79 kVAR C=174.7 µF XL=0.6075 Ω R=0.0015 Ω V=240 V |
| 3 | N/A | N/A | N/A | N/A | N/A |
| 4 | N/A | Q=66.37 kVAR C=764.1 µF XL=0.1389 Ω R=0.0015 Ω V=480 V | Q=53.33 kVAR C=614 µF XL=0.1728 Ω R=0.0015 Ω V=480 V | Q=48.32 kVAR C=556.4 µF XL=0.1907 Ω R=0.0015 Ω V=480 V | Q=3.79 kVAR C=174.7 µF XL=0.6075 Ω R=0.0015 Ω V=240 V |

Where Q is the capacitive reactive power, C is the capacitance, XL is the inductive reactance, and R is the resistance

### Table 7: Design data for PVS in each scenario

| Scenarios | Number of PVS modules | | | | | Arrays for each module | | | | |
|---|---|---|---|---|---|---|---|---|---|---|
| | PCC | BUS-3 | BUS-4 | BUS-5 | BUS-6 | PCC | BUS-3 | BUS-4 | BUS-5 | BUS-6 |
| 1 | 11 | N/A | N/A | N/A | N/A | S-21 P-5 | N/A | N/A | N/A | N/A |
| 2 | 10 | N/A | N/A | N/A | N/A | S-21 P-5 | N/A | N/A | N/A | N/A |
| 3 | N/A | 3 | 2 | 3 | 2 | N/A | S-21 P-5 | S-21 P-5 | S-21 P-5 | S-21 P-5 |
| 4 | N/A | 3 | 2 | 3 | 2 | N/A | S-21 P-5 | S-21 P-5 | S-21 P-5 | S-21 P-5 |

Where "S" refers to panels connected in series, and "P" refers to panels connected in parallel.

**Figure 4:** Power factor and power quality parameters in each scenario: (a) at the Point of Common Coupling (PCC), (b) at BUS_3, (c) at BUS_4, (d) at BUS_5, and (e) at BUS_6. Where: VV represents voltage variation, and VU represents voltage unbalance
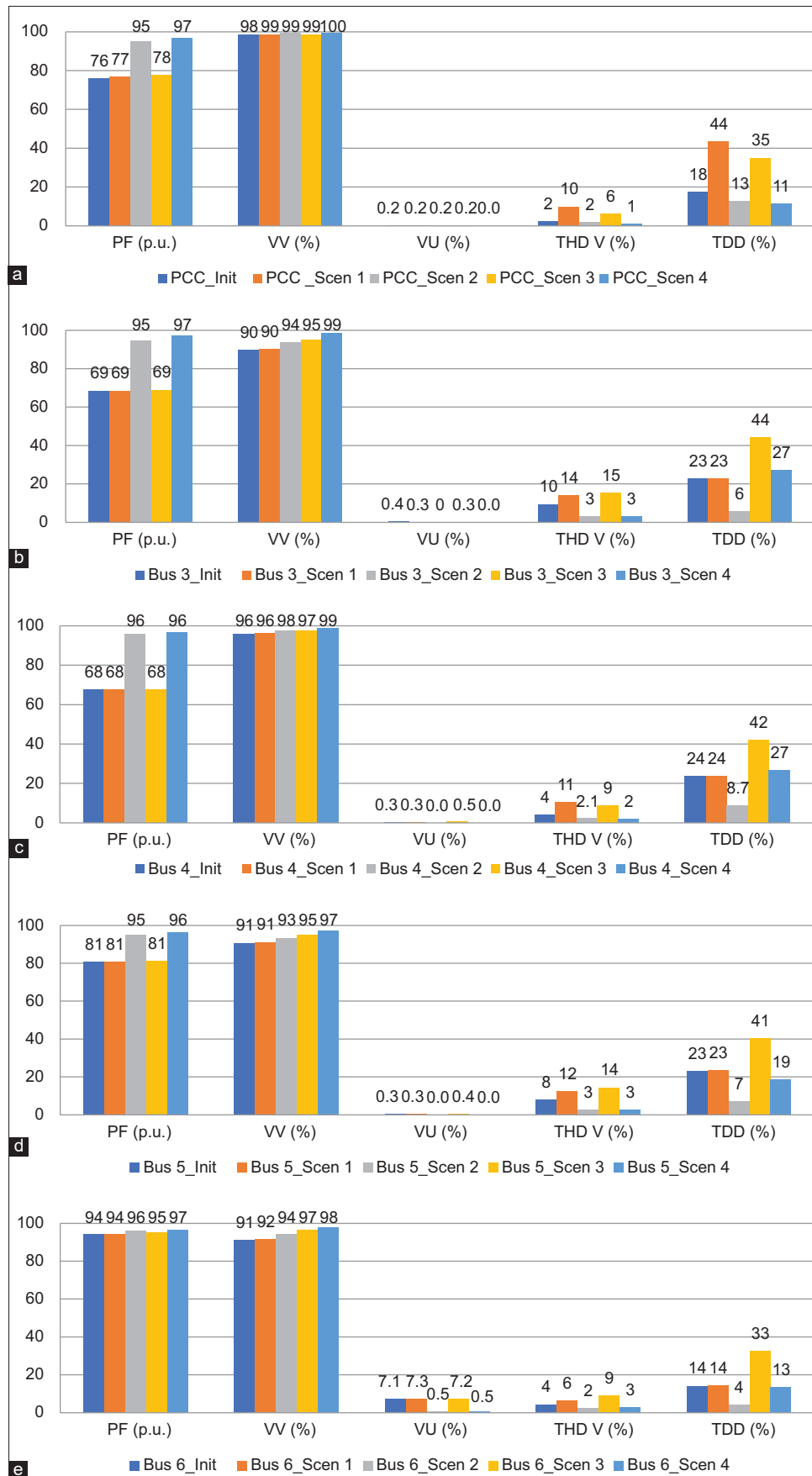
**Table 8: Costs and revenues of the evaluated scenarios in the case study**

| Parameters | Scen1 | Scen2 | Scen 3 | Scen 4 |
|---|---|---|---|---|
| Ko (COP) | 1,485,000,000 | 1,559,117,080 | 1,327,274,402 | 1,559,117,080 |
| Cost-Et (COP/Año) | 1,826,276,595 | 1,783,898,273 | 1,775,422,609 | 1,736,766,707 |
| Cost-Eloss (COP/Año) | 326,941,081 | 284,562,760 | 276,087,095 | 237,431,194 |
| Cost-OM (COP/Año) | 594,000 | 623,647 | 530,910 | 623,647 |
| Cost-R (COP) | 852,467 | 937,713 | 852,467 | 937,713 |
| Income-PVS (COP) | 619,466,928 | 605,092,343 | 602,217,426 | 589,105,473 |
| Income-SP (COP) | 62,503,111 | 41,699,009 | 77,165,188 | 55,287,848 |

Where: Cost-Et is the cost for total energy consumption in the IES, Cost-Eloss is the cost for energy losses, Cost-OM is the operation and maintenance cost, Cost-R is the replacement cost, Income-PVS is the income from energy consumption from the PVS, and Income-SP is the income from selling surplus energy delivered to the electrical grid

**Figure 5:** Energy: Consumed in the IES, consumed in the loads, consumed by Joule losses and PQ issues, generated, and consumed by PVS, and delivered as surplus to the grid. Where: Et is the total energy consumption in the IES, Eload is the energy consumption by the loads, Eloss is the energy due to losses, EG-PVS is the energy generated by the PVS, EC-PVS is the energy consumed by the PVS in the IES, and E-SP is the surplus energy from the PVS delivered to the electrical grid
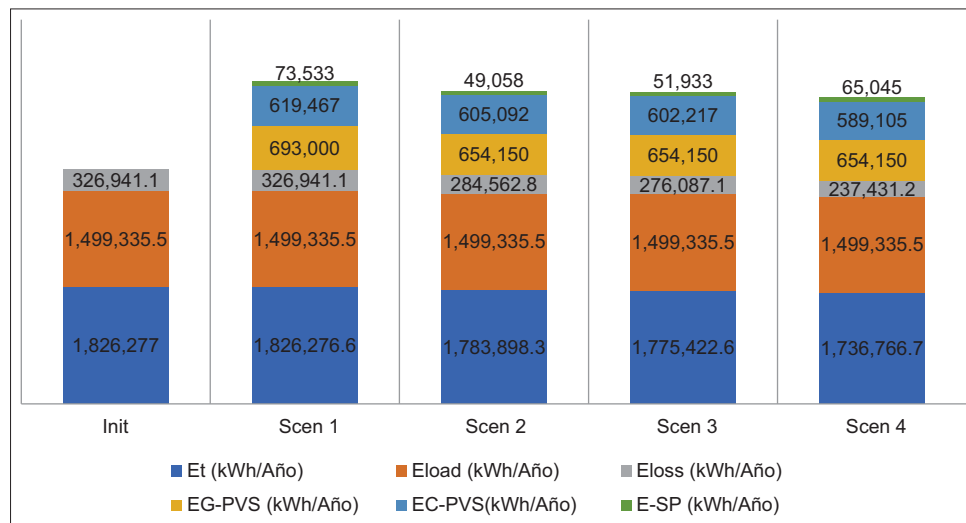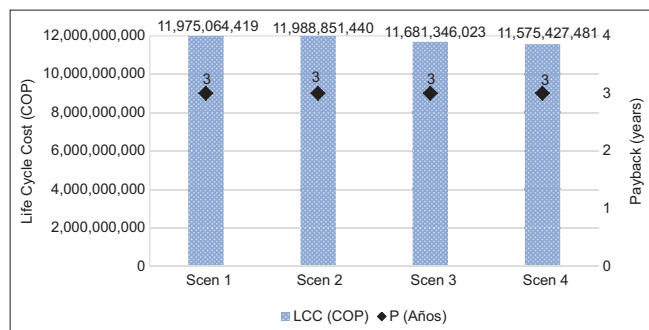


**Figure 6:** Life cycle cost and payback period for each scenario. Where P is the payback period



For the economic feasibility evaluation, a project lifespan of 25 years (Ndwali et al., 2020) was considered, with a discount rate of 12% (Datosmacro.com, 2024). The cost of surplus energy generated by PVS that can be sold to the electrical supply company is 850 COP/kWh (XM, 2024).

The Figure 6 shows that the difference between Scenario 4 with the lowest LCC and Scenario 1 with the highest LCC is only 3.3%, and the investment is recovered in the same period (3 years) in all scenarios, making it an economically attractive proposal. These

results are attributed to the fact that, although Scenario 4 presents the lowest costs for energy consumption (1,736,766,707 COP/year) and energy losses (237,431,194 COP/year), it also incurs the highest investment costs due to the use of equipment to mitigate power quality issues (1,559,117,080 COP). Additionally, the fact that Scenario 4 has the lowest energy consumption from the PVS results in lower project income from the use of renewable energy.

The study demonstrates that the use of conventional inverters in PVS projects can generate or exacerbate PQ issues such as harmonics. Furthermore, if PVSs are distributed near loads instead of being concentrated at the PCC, energy losses and consumption in the system can be significantly reduced, requiring the installation of lower capacity in PVS. This benefit increases if PQ issues are mitigated or avoided using pure sine wave inverters, harmonic filters, and other equipment for this purpose.

In the economic analysis, it was paradoxically observed that, while measures should be taken to reduce losses and energy consumption in a PVS, the lower the energy consumption of a PVS, the fewer economic benefits can be obtained from PVS. Additionally, reducing energy losses through technology-driven measures results in increased expenses that affect the feasibility of PVS installation projects.

Considering that several factors influence PVS design, such as replacing energy consumption from the grid, PQ, energy losses, concentrated or distributed generation, and associated costs with advantages and disadvantages in each case, it is recommended to include hierarchical analysis processes (Rocha et al., 2023), (Moreno et al., 2022) for decision-making in the evaluations of these projects.

## 4. CONCLUSION

In this study, a comprehensive methodology for the design of PVS in IES has been developed and presented, with a distinctive focus on PQ. This approach becomes essential in a context of continuous growth in PVS power generation, where the need to address potential deterioration of PQ becomes a crucial aspect.

The proposed methodology consists of 10 steps, ranging from interviews with interested companies to the technical, energy, and economic evaluation of the project. The novelty of this methodology lies in its multifactorial approach, using an Excel application in conjunction with the electrical modeling software ETAP. This enables a comprehensive assessment, considering common factors in PVS designs, such as load and supplied energy graphs, along with more specific aspects of IES operation, such as PVS placement, PQ, energy losses, and associated costs.

The validation of the methodology in an IES with initial PQ problems revealed that the worst technical and energy scenario occurred when PVS were installed at the PCC without mitigating PQ issues. In contrast, the most favorable technical and energy scenario was achieved with distributed installation on load buses, implementing actions to mitigate PQ problems through pure sine wave inverters, harmonic filters, and load balancing. This latter scenario resulted in substantial improvements, including a 5% reduction in energy consumption and a 27% reduction in energy losses.

Despite technical and energy improvements, the economic feasibility assessment revealed a 3-year payback period in all scenarios due to higher costs associated with mitigating PQ problems. Paradoxically, it was observed that reducing losses and energy consumption in an IES can limit the economic benefits derived from PVS implementation.

An additional conclusion highlights the complexity of PVS design, influenced by various factors such as grid consumption substitution, PQ, energy losses, and concentrated or distributed generation. The inclusion of hierarchical analyses in future studies, based on expert criteria, is suggested to enhance the decision-making process in the design of photovoltaic systems in industrial settings. These conclusions underscore the importance of comprehensively addressing the challenges associated with PVS implementation in IES.

## 5. ACKNOWLEDGMENTS

## REFERENCES

Abril, I.P. (2012), Cálculo de parámetros de filtros pasivos de armónicos calculation of the harmonics passive filters parameters. Ingeniería Energética, 33(2), 20-29.

Adefarati, T., Bansal, R.C. (2019), Reliability, economic and environmental analysis of a microgrid system in the presence of renewable energy resources. Applied Energy, 236, 1089-1114.

Ahmad, T., Zhang, D., Huang, C., Zhang, H., Dai, N., Song, Y., Chen, H. (2021), Artificial intelligence in sustainable energy industry: Status Quo, challenges and opportunities. Journal of Cleaner Production, 289, 125834.

Ali, B., Attayyab Khan, A., Ahmed Khan, Q., Yamin, T., Adeel, M. (2019), Portable Solar Powered DC Pumping System Using Pump Jack and MPPT. In: 2019 2nd International Conference on Computing, Mathematics and Engineering Technologies, ICOMET.

Al-Karakchi, A.A.A., Nashad, F.E., Putrus, G., Foti, S., Smith, D., Elsdon, M. (2019), Cost-Effective Integration System of Solar Cell Powered Remote Small-Size Wireless Communication. In: 2nd International Conference on Electrical, Communication, Computer, Power and Control Engineering, ICECCPCE 2019.

Angarita, E.N., Zambrano Mejía, A., Santos, V.S., Daniel Donolo, P. (2023), Assessment of Electrical Power Quality Parameters in an Industrial Electrical System. In: 2023 IEEE Workshop on Power Electronics and Power Quality Applications (PEPQA). p1-6.

Barbón, A., Carreira-Fontao, V., Bayón, L., Silva, C.A. (2023), Optimal design and cost analysis of single-axis tracking photovoltaic power plants. Renewable Energy, 211, 110.

Cabana-Jiménez, K., Candelo-Becerra, J.E., Sousa Santos, V., Vásquez-Carbonell, M. (2024), Power demand estimation techniques applied to microgrid. International Journal of Ambient Energy, 45(1), 2306201.

Charris, N.C., Santos, V.S., Eras, J.J.C. (2023), Aspects to consider in the evaluation of photovoltaic system projects to avoid problems in power systems and electric motors. International Journal of Energy Economics and Policy, 13(3), 334-341.

Choudhury, S. (2022), Review of energy storage system technologies integration to microgrid: Types, control strategies, issues, and future prospects. Journal of Energy Storage, 48, 103966.

Corporación de Desarrollo Tecnológico-Cámara Chilena de Construcción. (2013), Dimensionamiento de Sistemas Solares Fotovoltaicos Conectados a Red. Chile: Impresos Jemba. Available from: https://www.cdt.cl/download/76553

CREG. (2018), Resolución CREG 015-2018. Metodología Para la Remuneración de la Actividad de Distribución de Energía Electrica en el Sistema Interconectado Nacional. In Resolución. Vol. 15. Belgium: CREG. p239.

Datosmacro.com. (2024), Tipos del Banco Central de Colombia. Available from: https://datosmacro.expansion.com/tipo-interes/colombia

Global Status Report. (2021), Renewables 2021 global status report. In: Global Status Report for Buildings and Construction: Towards a Zero-Emission, Efficient and Resilient Buildings and Construction Sector.

Habib, S., Liu, H., Tamoor, M., Zaka, M.A., Jia, Y., Hussien, A.G., Zawbaa, H.M., Kamel, S. (2023), Technical modelling of solar photovoltaic water pumping system and evaluation of system performance and their socio-economic impact. Heliyon, 9(5), e16105.

ICONTEC. (2008), NTC 5001:2008-Calidad de la Potencia Eléctrica. Límites y Metodología de Evaluación en punto de Conexión Común. Colombia: ICONTEC.

ICONTEC. (2013), NTC 1340-Electrotecnia. Tensiones y Frecuencia Nominales en Sistemas de Energía Eléctrica en Redes de Servicio Público. Colombia: ICONTEC.

IEEE. (2014), IEEE Std 519™-2014: IEEE Recommended Practice and Requirements for Harmonic Control. In: ANSI/IEEE Std. 519. Vol. 2014. United States: IEEE. p. 5-9.

IEEE. (2019), IEEE Std 1159™-2019: IEEE Recommended Practice for Monitoring Electric Power Quality. In: IEEE Standard 1159-2019 (Revision of IEEE Std 1159-2009). Vol. 2019. United States: IEEE. p. 1-98.

Jamil, E., Hameed, S., Jamil, B., Qurratulain. (2019), Power quality improvement of distribution system with photovoltaic and permanent magnet synchronous generator based renewable energy farm using static synchronous compensator. Sustainable Energy Technologies and Assessments, 35, 98-116.

Khare, V., Nema, S., Baredar, P. (2016), Solar-wind hybrid renewable energy system: A review. Renewable and Sustainable Energy Reviews, 58, 23-33.

Koholé, Y.W., Wankouo Ngouleu, C.A., Fohagui, F.C.V., Tchuen, G. (2023), Quantitative techno-economic comparison of a photovoltaic/wind hybrid power system with different energy storage technologies for electrification of three remote areas in Cameroon using Cuckoo search algorithm. Journal of Energy Storage, 68, 107783.

Moreno, C., Ospino-Castro, A., Robles-Algarín, C. (2022), Decision-making support framework for electricity supply in non-interconnected rural areas based on FAHP. International Journal of Energy Economics and Policy, 12(5), 79-87.

Naderipour, A., Kamyab, H., Klemeš, J.J., Ebrahimi, R., Chelliapan, S., Nowdeh, S.A., Abdullah, A., Hedayati Marzbali, M. (2022), Optimal design of hybrid grid-connected photovoltaic/wind/battery sustainable energy system improving reliability, cost and emission. Energy, 257, 124679.

Nasir, J., Javed, A., Ali, M., Ullah, K., Kazmi, S.A.A. (2023), Sustainable and cost-effective hybrid energy solution for arid regions: Floating solar photovoltaic with integrated pumped storage and conventional hydropower. Journal of Energy Storage, 74, 109417.

Ndwali, K., Njiri, J.G., Wanjiru, E.M. (2020), Multi-objective optimal sizing of grid connected photovoltaic batteryless system minimizing the total life cycle cost and the grid energy. Renewable Energy, 148, 1256-1265.

Ren, S., Hao, Y., Xu, L., Wu, H., Ba, N. (2021), Digitalization and energy: How does internet development affect China's energy consumption? Energy Economics, 98, 105220.

Ren, Y., Jin, K., Gong, C., Hu, J., Liu, D., Jing, X., Zhang, K. (2023), Modelling and capacity allocation optimization of a combined pumped storage/wind/photovoltaic/hydrogen production system based on the consumption of surplus wind and photovoltaics and reduction of hydrogen production cost. Energy Conversion and Management, 296, 117662.

Rocha, C.M.M., Pertuz Ortiz, J.D., Rodriguez Ibanez, N.A. (2023), A diffuse analysis based on analytical processes to prioritize barriers in the development of renewable energy technologies in alignment with the united nations sustainable development goals: Evidence from Guajira/Colombia. International Journal of Energy Economics and Policy, 13(4), 481-495.

Roy, S., Dev Shukla, R., Chakrabarti, R., Nath, S., De, A., Pandev, A. (2019), Cost Effective Design Control of DC-DC Converter for Solar PV System with MPPT. UEMGREEN 2019-1st International Conference on Ubiquitous Energy Management for Green Environment.

Saqib, M.A., Saleem, A.Z. (2015), Power-quality issues and the need for reactive-power compensation in the grid integration of wind power. Renewable and Sustainable Energy Reviews, 43, 51-64.

Sharma, B., Dahiya, R., Nakka, J. (2019), Effective grid connected power injection scheme using multilevel inverter based hybrid wind solar energy conversion system. Electric Power Systems Research, 171, 1-44.

Sinha, S., & Chandel, S. S. (2017). Improving the reliability of photovoltaic-based hybrid power system with battery storage in low wind locations. Sustainable Energy Technologies and Assessments, 19. https://doi.org/10.1016/j.seta.2017.01.008

Tutiempo Network, S.L. (n.d.), Radiación Solar En Barranquilla. Available from: https://www.tutiempo.net/radiacion-solar/barranquilla.html

XM. (2024), Sinergox. Available from: https://sinergox.xm.com.co/paginas/home.aspx

Yang, M., Alballa, T., Khalifa, H.A.E.W. (2023). A comprehensive data analytics framework for risk management in photovoltaic system design projects. Optik, 295, 171411.

Zidane, T.E.K., Adzman, M.R., Zali, S.M., Mekhilef, S., Durusu, A., Tajuddin, M.F.N. (2019), Cost-effective topology for photovoltaic power plants using optimization design. Proceeding-2019 IEEE 7th Conference on Systems, Process and Control, ICSPC 2019.